EARTH SCIENCES
RESEARCH JOURNAL
Earth Sci. Res. J. Vol. 26, No. 1 (March, 2022): 55 - 68

UNIVERSIDAD NACIONAL DE COLOMBIA

MINERALOGY

Mineralogy and geochemical signatures as indicators of differential weathering in natural soil profiles from the West Asturian-Leonese Zone (NW Iberia)

Sara Alcalde-Aparicio, M. Vidal-Bardan, E. Alonso-Herrero
Universidad de León, España.
salca@unileon.es

ABSTRACT

This paper presents detailed mineralogical results together with a geochemical characterization for a sequence of six natural soil profiles. Bedrock samples (R series) and overlying soil samples (S series) were characterized. The soil profiles are distributed in a series of Paleozoic lithological units from lower Ordovician to upper Carboniferous in age (Iberian Massif, NW Iberia). The lithological influence on mineral properties and geochemical composition and, how different weathering may be occurring under very similar temperate and acidic conditions, have been studied. Field observations together with laboratory analyses were indicative of differential weathering. So, a series of selected chemical indices and relations were applied to clarify this assumption. The mineralogy was analysed by Scanning electron microscopy (SEM-EDS), X-ray diffraction (XRD) of rock powder and soil oriented aggregates. X-ray fluorescence spectrometry (XRF) and inductively coupled plasma mass spectroscopy (ICP-MS) were applied to analyse chemical composition. The first results showed how major elements, SiO_2, Al_2O_3 and Fe_2O_3, slightly enriched in the soil profiles, are consistent with the dominant mineralogy: quartz, chlorite, muscovite and/or illite, together with kaolinite and albite. The bases K_2O, Na_2O, CaO and MgO are also coherent with mineral composition and experience little variation, but are gradually removed in the profiles. The mobility of major elements leads to a general loss of bases and, in general, a slight enrichment in silica and sesquioxides. SiO_2 is enriched, firstly accumulated in soils and partially depleted by dissolution as colloidal form. Al_2O_3 in some soils is slightly less than in former rocks, so other physical processes are expected to take place, involving clay removal with consequent aluminium depletion too. A special emphasis has been given to albite coexisting with kaolinite, firstly supposed to be directly inherited from parent substrates when present, but finally the chemical index PIA shows it was mainly due to mineral alteration of plagioclases. The best correlations to explain the albite alteration and kaolinitization progress were obtained with chemical indices PIA, CIW, CIA and Al_2O_3/Na_2O ratio. This together with mineralogical signatures, suggest that kaolinite is the result of gradual dissolution due to the acid hydrolysis of albite in such acidic environments, which may also be attributed to the organic matter influence.

Keywords: geochemical relations; soil profiles; differential weathering; Plagioclase Index of Alteration (PIA); albite acid hydrolysis;

Mineralogía de arcillas y señales geoquímicas como indicadores rápidos de procesos de meteorización química diferencial en una litosecuencia silícea de perfiles de suelos

RESUMEN

Este trabajo presenta resultados mineralógicos detallados junto con una caracterización geoquímica para una secuencia de seis perfiles de suelos naturales. Se caracterizaron muestras de rocas (serie R) y muestras de suelos suprayacentes (serie S). Los perfiles de suelo se distribuyen en una serie de unidades litológicas paleozoicas de edad desde el Ordovícico inferior hasta el Carbonífero superior (Macizo Ibérico, NW de Iberia). Se ha estudiado la influencia litológica en las propiedades mineralógicas y en la composición geoquímica y cómo puede ocurrir una alteración diferente en los perfiles bajo condiciones templadas y ácidas muy similares. Las observaciones de campo junto con los análisis de laboratorio fueron indicativos de alteración diferencial. Por lo tanto, se aplicaron una serie de índices químicos de meteorización y algunas relaciones seleccionadas para aclarar esta suposición. La mineralogía se analizó mediante microscopía electrónica de barrido (SEM-EDS), difracción de rayos X (XRD) de muestras de polvo de roca y agregados orientados del suelo. Se aplicaron espectrometría de fluorescencia de rayos X (XRF) y espectroscopia de masas de plasma acoplado inductivamente (ICP-MS) para analizar la composición química. Los primeros resultados mostraron cómo los elementos mayoritarios, SiO_2, Al_2O_3 y Fe_2O_3, ligeramente enriquecidos en los perfiles de suelo, son consistentes con la mineralogía dominante: cuarzo, clorita, moscovita y/o ilita, junto con caolinita y albita. Las bases K_2O, Na_2O, CaO y MgO también son coherentes con la composición mineral y experimentan poca variación, pero se eliminan gradualmente en los perfiles. La movilidad de los elementos mayoritarios lleva a una pérdida general de bases y, en general, un ligero enriquecimiento en sílice y sesquióxidos. El SiO_2, primero se acumula en los suelos y se pierde parcialmente por disolución en forma coloidal. El Al_2O_3, en algunos suelos es ligeramente menor que en las rocas, por lo que se espera que parte se pierda también en forma coloidal o tengan lugar otros procesos físicos que involucran la remoción de la arcilla, con la consiguiente pérdida del aluminio también. Se ha dado un énfasis especial a la presencia de albita que coexiste con la caolinita; en primer lugar, se supone que se heredó directamente de los materiales originales en los que está presente, pero finalmente el índice PIA muestra que se debe principalmente a la alteración de las plagioclasas. Las mejores correlaciones para explicar esta alteración de la albita y el progreso de la caolinita, se obtuvieron con los índices químicos PIA, CIW, CIA y la relación Al_2O_3/Na_2O, que junto con firmas mineralógicas, sugieren que la caolinita es el resultado de la disolución gradual debido a la hidrólisis ácida de la albita en dichos ambientes ácidos, que también puede ser atribuido a la influencia de la materia orgánica.

Palabras Clave: relaciones geoquímicas, perfiles de suelo, alteración diferencial, Índice de Alteración de las Plagioclasas (PIA), hidrólisis ácida albita

Record
Manuscript received: 19/07/2019
Accepted for publication: 07/01/2022

How to cite item:
Alcalde-Aparicio, S., Vidal-Bardan, M., & Alonso-Herrero, E. (2022) Mineralogy and geochemical signatures as indicators of differential weathering in natural soil profiles from the West Asturian-Leonese Zone (NW Iberia). *Earth Sciences Research Journal*, 26(1), 55-68 . https://doi.org/10.15446/esrj.v26n1.81087

Introduction

The processes controlling the alteration of primary minerals depend on the relative mobility of some major components (Anderson & Hawkes, 1958; Johnson et al., 1968; White et al., 2001; Anderson et al., 2002; White & Brantley, 2003; Wilson 2004; Meunier et al., 2007; White & Buss, 2014). Basically, the unique genetic relationship between the soil and the parent material through the profiles helps to understand the role of rock weathering and soil formation. The influence of the parent material mineral composition on the genesis of the soils is still a question to be explored, as widely shown in the traditional literature (Chesworth, 1973a). Therefore, the main source of the bases is related to in situ chemical weathering of local bedrocks (Munroe et al., 2007). Special importance has been given to the removal of alkali and alkaline earth elements (Na, Ca, Mgand K) during the continental weathering (Chesworth, 1973b), due to the alteration of clay minerals and a high removal of Na from dissolution of feldspars and plagioclases, followed by a progressive enrichment in silica and Al and Fe sesquioxides (Wilson, 2004); occasionalyy, desilification occurs at the final weathering stage. During weathering the rock forming primary minerals, micas and feldspars, are depleted in bases; in this way, K release is considered a good measure of the degree of alteration of the aluminium silicate minerals (Wilson, 2004). In addition, chemical weathering of silicate rocks through acid hydrolysis could take place and lead to an exchange of Na, K, Ca and Mg for H and, perhaps, a loss of Si (Bain et al., 1990; Ezzaım et al., 1999a, 1999b; Papoulis et al., 2004). According to Banfield & Eggleton (1990). Both processes, the loss of K and Na and the enrichment in Al, are in consonance with an advancing process of kaolinization and formation of iron and aluminium oxyhydroxides too. This fact has been explained by some authors for weathering soil profiles from the Iberian massif (Molina et al., 1990; Vicente et al., 1991; Vicente et al., 1997; Molina & Cantano, 2002; Jiménez-Espinosa et al., 2007; Núñez & Recio 2007; Fernández-Caliani & Cantano 2010; Doval et al., 2012).

Other relevant factors regarding weathering in the traditional literature include the fundamental alteration mechanisms and the products derived from the primary minerals (Banfield & Eggleton, 1990; Merriman et al., 1990; Robertson & Eggleton, 1991; Robert & Tessier, 1992; Gardner & Walsh, 1996; Aspandiar & Eggleton, 2002, Spears, 2016). Many secondary clays are commonly considered an alteration product in acidic soil environments as explained by Pédro (1997). For example, the evolution of parent rocks controlled by an hydrolysis phenomenon, including bisialitisation, monosiallitisation and allitisation, within the formation of minerals from the smectite group, kaolinite group gibbsite and iron oxides group found in the pedological horizons. Evaluating geochemical composition, not only releases basic information about the formation conditions, but also the evolution and the alteration stages of the rock substrates and soils. Wilson (2004) noted that the differences in alteration mechanisms, products and the rates of weathering commonly observed among bedrock and soil environments can differ widely, even in the same geological units. Nesbitt et al. (1980) already mentioned degradation and leaching dominate the early weathering stages, whereas during the advanced stages, ion exchange and adsorption onto clays are of most influence. Banfield & Eggleton (1990), Fedo et al. (1995) and Price & Velbel (2003) suggested a sequential formation of secondary weathering products and pointed out the utility of evaluating weathering indices attending to simple profile depth variations. Thus, evaluating chemical weathering indices and element relations between mobile or immobile elements help rapidly to understand weathering intensity, possible processes and, sometimes, soil grade of development and evolutionas proven for instance by Gardner & Walsh (1996**)**. The main chemical alteration indices (Ruxton 1968; Parker 1970; Nesbitt and Young 1982; Harnois 1988; Jayawardena and Izawa 1994; Fedo et al. 1995) have deeply contributed to the understanding of weathering a great variety of geological substrates. Even though, some of the conventional indices, mainly use to estimate weathering intensity, should be reformulated as an alternative approach to evaluate different rock weathering grades (Guan et al., 2001; Meunier et al., 2013). Nevertheless, chemical indices of alteration resulted really helpful when evaluating the losses or enrichment of base cations from the rocks However, evaluating the release of silica and relative accumulation of iron and aluminum in soils from the rock weathering requires being adapted (Meunier et al., 2013).

Additionally, several studies highlighted implications for paleoweathering conditions and provenance as pointed out by Fedo et al. (1995). Recent reviews on climatic and geochemistry (Perri, 2020 or Dinis et al., 2020) enlighten their strongly interactions using chemical indices as proxies. Recently, Dinis et al. (2020) have recognised these significant relationships between mineralogical and geochemical signatures of sediments and rainfall registers at catchment scale. Moreover, some other factors take an important role in such complex context, particularly diverse physical factors driven by topography as suggested by Tardy et al. (1973).

This work characterizes the mineralogical and geochemical composition of a series of six natural profiles consisting of soils (S series) and parent rocks (R series) developed on Palaeozoic lithologies from the Iberian Massif under similar weathering conditions in temperate and acidic environments. The influence of lithology on mineral and geochemical properties and the assumption of mineral alteration by differential weathering have been addressed. The specific aims of this research are: 1) characterize the major compositional mineralogy, particularly focusing on fine-grained and clay fractions in six selected weathering profiles; 2) identify the geochemical signatures according to the chemical indices of alteration; 3) understand the factors controlling the weathering processes and 4) explain possible differential chemical weathering mechanisms presumably taking place in such acidic environments.

Geological setting

The profile sites studied are located in the NW part of the Iberian Massif (Variscan Orogenic Belt) included in the West Asturian–Leonese Zone (WALZ) (Figure 1), specifically in the Navia-Alto Sil Domain (NASD) (Pérez-Estaún et al., 2004; Marcos et al., 2004). The Variscan Orogeny in the WALZ was a polyphasic deformative process associated with synkinematic metamorphism under epizonal deformation conditions, mainly to greenschist facies (Martínez-Catalán et al., 1990; Suárez et al., 1990), with mineral paragenesis associations typical of the chlorite zone. The WALZ, including the Lower to Upper Paleozoic units, is characterized principally by the presence of a thick assemblage of Cambrian-Ordovician siliciclastic rocks, which shows an overall structure, formed largely by recumbent folds and thrusts.

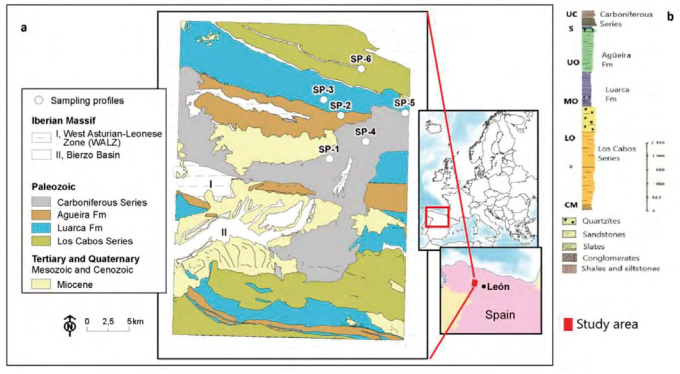

Figure 1. Weathering sampling profiles (SP-1, SP-2, SP-3, SP-4, SP-5, SP-6) a) location in the lithological units from the WALZ (NW Iberian Massif, Spain). b) Synthetic stratigraphic column modified from Pérez-Estaún (1990) showing formations and series form ages UC: Upper Carboniferous; S: Silurian; UO: Upper Ordovician; MO: Middle Ordovician; LO: Lower Ordovician and CM: Cambrian.

Map source: The National Geological Survey Institute of Spain (IGME) modified from Rodríguez Fernández (1982).

The lithostratigraphic sequence starts with the Lower Paleozoic materials of Cambrian to Ordovician age (Pérez-Estaún et al., 1990). It begins with detritic facies characterized by an alternation of quartzites with slates, siltstones and sandstones referred to as the Los Cabos Series (Cua). A range of later Paleozoic materials, referred to as the Transition Layers, gradually gives way to the Luarca Formation (Lua), an assemblage of fine grained black slates, rich in sulphides like pyrite and organic matter. This is immediately followed by the Agüeira Formation (Agu), formed by alternating sandstones, siltstones and shales with a presence of turbidite depositional environment, which sometimes culminates in a quartzite layer. The Silurian strata, poorly represented, are found in a gradually alternating section, including fully sandy phases with varying proportions of slates. These

are discordantly overlain by Upper Carboniferous (Carb) (Stephanian B-C) synorogenic materials of the El Bierzo coal basin (Barba et al., 1994), which represent the development of a strong paleorelief. The Carboniferous unit consists of a broad range of sediments such as alternating layers of sandstones, shales, siltstones and conglomerates combined with intermediate coalbed deposits (Colmenero et al., 2002; Wagner, 2004).

Materials and methods

The sampling profiles (SP) are located in six different lithostratigraphic units within the Paleozoic succession named as Cua, Lua, Agu and Carb (Table 1): Los Cabos Series (SP-6)-Cua, Luarca Formation (SP-3 and SP-5)-Lua, Agüeira Fm (SP-2)-Agu, and Carboniferous Series (SP-1 and SP-4)-Carb. Samples including partially weathered or fresh rocks (R-series) were named as: R1 (Figure 2a), R2 (Figure 2e) , R3 (Figure 2b), R4 (Figure 2f), R5 (Figure 2g) and R6 (Figure 2h); other altered weathered geological materials in contact with the bedrocks beneath, including the soil (S-series) named as: S1 (Figure 2a), S2.1 and S2.2 (Figure 2e), S3.1 and S3.2 (Figure 2b), S4 (Figure 2f), S5 (Figure 2g), S6 (Figure 2h), were collected in the sampling sites from SP-1 to SP-6 as showed in Figure 1.The correspondence between the profile sites and samples series is specified below (Table 1): SP-1 (samples R1 and S1)-Carb; SP-2 (samples R2, S2.1 and S2.2)-Agu; SP-3 (samples R3, S3.1 and S3.2)-Lua, SP-4 (samples R4 and S4)-Carb; SP-5 (R5 and S5)-Lua; SP-6 (R6 and S6)-Cua.

Table 1. Descriptive features of the investigated sampling profiles soil horizons (S-series) and bedrocks samples (R-series) location (UL: Upper and LL: Lower Level of weathering) according to depth, general profile weathering degree descriptive material features (HD: high; MD: moderate, LD: low degree), lithological units, parent rocks and soil series. **Acronym for the geological unit's name*

Profile site	U.T.M. Coordinates (29N)	Sample	Rock/Soil Horizon	Depth (cm)	Level of weathering	Weathering degree	Geologic System/ Formation	Lithological Unit*	Parent material	Soil Series
SP-1	X:721.188.6 Y:4.730.234.5	R1	R	+18	LL	HD	Carboniferous	Carb	Beige Argillite	Carb-Boeza
		S1	Ah	0-18	UL					
SP-2	X:722.255.7 Y:4.735.448.2	R2	R	+ 25	LL	MD	Agüeira	Agu	Sandy Slates and Grey siltstones	Agu-Igüeña
		S2.1	Ah1	0-8	UL					
		S2.2	Ah2	8-25	UL					
SP-3	X:720.118.1 Y:4.737.203.2	R3	R	+ 20	LL	HD	Luarca	Lua	Black slates and shales	Lua-Urdiales
		S3.1	Ah	0-12	UL					
		S3.2	A/R	12-20	UL					
SP-4	X:725.378.6 Y:4.732.542.95	R4	R	+25	LL	MD	Carboniferous	Carb	Sandstones and Sandy siltstones	Carb-Rodrigatos
		S4	Ah	0-25	UL					
SP-5	X:729.825.63 Y:4.736.191.3	R5	R	+15	LL	MD	Luarca	Lua	Black slates and shales	Lua-Tremor
		S5	Ah	0-15	UL					
SP-6	X:722.500.26 Y:4.740.380.14	R6	R	+15	LL	LD	Los Cabos Series	Cua	Quartzites	Cua-Colinas del Campo
		S6	Ah	0-15	UL					

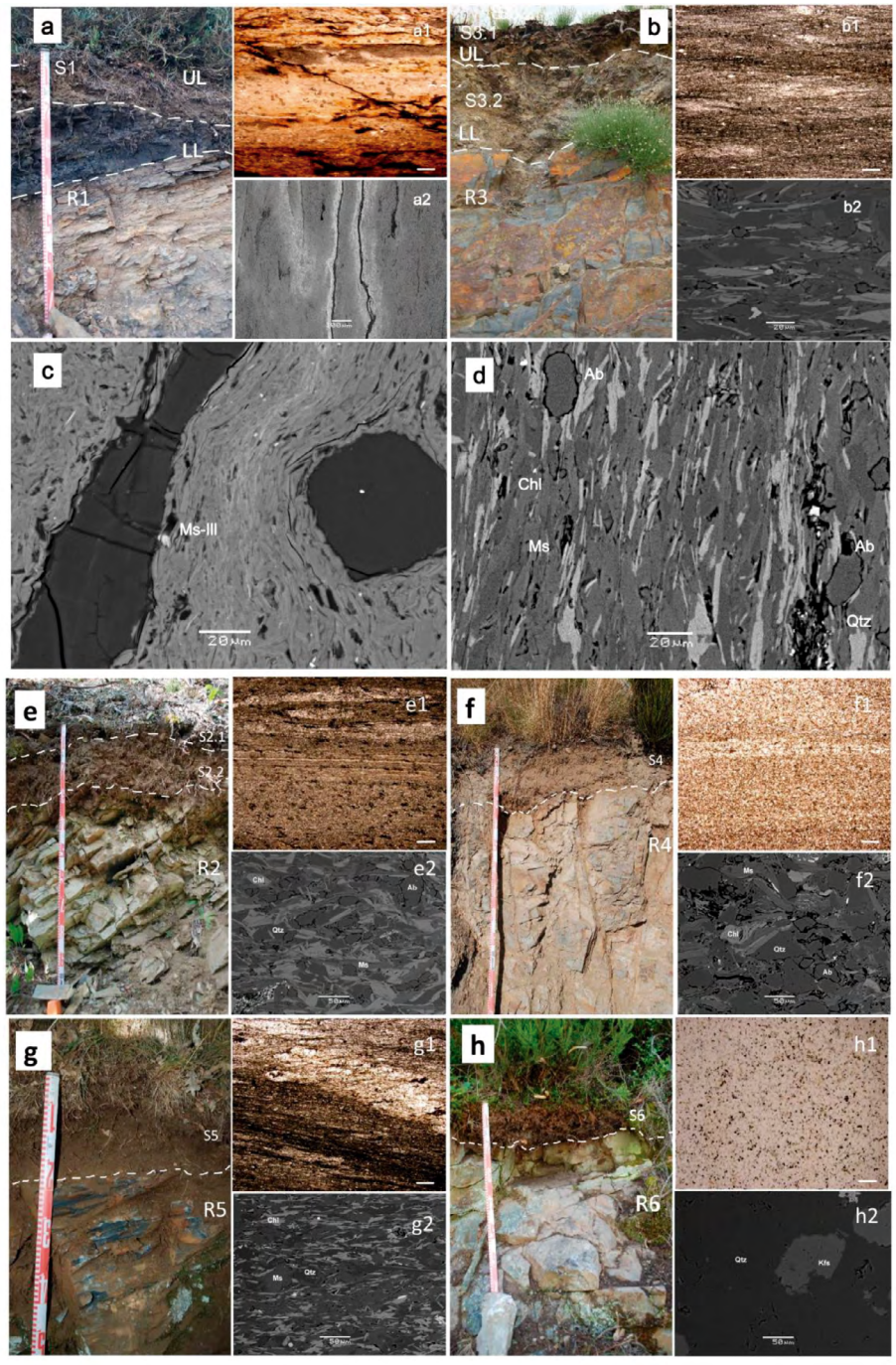

Figure 2. Soil profiles showing two different levels of weathering UL: upper level; LL: lower level where samples were taken: image a) profile SP1 (S1 and R1) and image b) profile SP3 (S 3.1, S3.2 and R3). Images from e) to h) soil profile sites SP2, SP4, SP% and SP6 respectively. Thin sections showing the rock samples microtextures and granulometry R1 (image a1) and R3 (image b1); R2 (image e1), R4 (image f1), R5 (image g1) and R6 (image h1). Observational scale at 1 mm. SEM BSE images (a2 at 100 µm and b2 at 20 µm captured scale; e2, f2, g2 and h2 at 50 µm captured scale) SEM BSE detailed images for identification of muscovite (Ms) and illite (Ill) on R1 (image c) and quartz (Qtz), muscovite (Ms), chlorite (Chl) and albite (Ab) on R3 (image d).

Microscopy

Scanning electron microscopy with energy dispersive X-ray spectrometry (SEM-EDS) was carried out as a supporting tool to validate mineral petrographic analysis. Thin sections from sample substrates were previously studied by optical microscopy (POM, transmitted and reflected light), using a Nikon Eclipse E600 POL petrographic microscope. The same polished thin sections were subsequently carbon coated and studied under a JEOL JSM-6480 high resolution scanning electron microscope (SEM), equipped with an Oxford Instruments D6679 Energy Dispersive X-ray Spectrometry (EDS) detector. For each specimen acceleration voltages range of 10 to 20 keV, working distance was 10 mm and count rate set at 15000 counts/s. Back-scattered electron (BSE) images were acquired and processed using INCA Energy Software provided by Oxford Instruments.

X ray diffraction

Representative portions of powdered rock samples were subjected to X-ray diffractometric analyses. Air dried rock samples were pulverized in a Restch PM400 automatic rotary planetary mortar mill, collecting the fraction

<125 µm. XRD analyses were performed at room temperature and 400 C during 0.75 hours. Representative samples were subjected to X-ray powder diffraction, using a SIEMENS Bruker D5000 series diffractometer system equipped with Cu-K-alpha radiation at 40kV and 30 mA, 0.2 mm receiving slit, a range of 2°-58° 2θ and graphite secondary monochromator facilities. Scanning step size was set at 0.02 º 2θ and the scanning rate 1 second per step, giving a scan speed of approximately 2º 2θ per minute and a total duration of 0.75 h.

Oriented aggregates of the <2.0 µm fine clay fraction were obtained from the soil samples, using suspension after hexametaphosphate dispersion, separation by sedimentation and settling techniques after 24 hours (Klug & Alexander, 1974). The clay samples were dried at 40°C, homogenized and manually powdered using an agate pestle and mortar. Previously, the sample pretreatment was the organic matter removal with a hydrogen peroxide agent (30% v/v) at 25 C. Duplicate samples were mixed and shaken in a tapered centrifuge tube. The remainder, which stayed in suspension, was removed and dropped on to a circular glass slide. This was then allowed to dry in the laboratory atmosphere, leaving an oriented clay film on the surface of the glass slide. Each glass slide, with its clay film, was subjected to X-ray diffraction analysis using a Panalytical Empyrean II diffractometer in the air-dried state, using Cu-K-alpha radiation and in this case a range of 2°-46° 2θ for soil clay samples. The slides were then placed in a desiccator containing ethylene glycol, and exposed to the glycol vapour at room temperature for several days. The glycol-treated slides were then heated at 400 C for one hour and subjected to XRD analysis. Identification of the minerals in the parent rocks and soil clays was carried out following the general indications of Moore & Reynolds (1989).

Chemical analyses

Chemical analyses were performed within duplicated samples including bulk chemistry and fine grained fractions <2.0 µm for clay soil samples. Major element analyses were carried out by X ray fluorescence spectrometry (XRF) and, alternatively, some of the major and minor elements were measured by Inductively Coupled Plasma Mass Spectrometry (ICP-MS). The fused borosilicate disks were prepared with 95%Pt/5%Au crucibles, adding 0.500 g of a 1:1 mixed fusion flux of Lithium tetraborate/metaborate (50% $Li_2B_4O_7$/50% $LiBO_2$), in a fusion melting induction furnace heated to 1000 ºC during 20 min, using a non-wetting agent of LiBr. They were analysed in a BRUKER-NONIUS S4 Pioneer wavelength dispersive XRF spectrometer. The samples prepared following the specifications of the alkali fusion technique required acid dissolution with HNO_3 5% (v/v). They were measured by ICP-MS in a Thermo Scientific quadrupole XSeries2, with detection limits of 0.01% using as standard elements In, Sc and Rh. The major element oxides CaO, MgO, Na_2O, K_2O, SiO_2, Fe_2O_3, Al_2O_3, P_2O_5, MnO and TiO_2 were expressed as weight percentages (wt %). Previously, representative splits of each sample were oven-dried, and then heated at 975 C for 12h in a high temperature furnace HOBERSAL12-PR400to obtain the Loss on Ignition (LOI) percentage in each case.

Results

Mineralogy

In the preliminary mineralogical identification for rocks the principal minerals are phyllosilicates of the mica group, mostly Ms-Ill (Figure 2c) and chlorites (Figure 2d) respectively, accompanied by quartz (3.34 Å) and feldspars, according to the major peaks (3.19 Å and 3.22-3.24 Å) correspond to plagioclases (albite) as confirmed by SEM analyses (Figure 2d) or K-feldspars, in the case of R6 (Figure 2h2). The microscopic and SEM BSE analyses can be found detailed on Figure 2. It can be noted that albite is present on R3, R5 and R4 (Figures b2, f2 and g2) and, clearly more abundant, on R2 (Figure e2), all assessing the XRD analyses too.

In addition, kaolinite (Kln) is only present in some of the R-samples (Table 2). There is a relative higher abundance of chlorite in samples R3, R5 and R2, the albite content is higher in R2, however kaolinite content is higher in R1 (Table 2). The major minerals in the sample R1 are mica (muscovite-illite), quartz and kaolinite respectively (Ms-Ill, Qtz and Kln) as seen in Figure 3. Kaolinite is clearly identified in sample R1 (Figure 3a). By contrast, an iron-rich chlorite identified in samples R2 to R5 as shown in (Figure3b), SEM analysis confirm that correspond to chamosite (Figure 3b). From samples R2 to R6 the peaks at 10 Å and 5.0 Å in all patterns analysed are indicating mica, but finally the SEM results shown enough evidence to be identified as muscovite, so it was also confirmed by SEM. It is noted that the peak of 3.34 Å can be also of mica-illite, so the reflection of 4.26 Å would be enlightening. This also applies to sample R1 (Figure3a), although overall intensity is relatively low for that pattern, suggesting a mica (muscovite) rather than a less well-ordered illite phase as confirmed by SEM analysis (Figure 2c).

Table 2. Mineral identification in the rock samples and relative mineral abundance referred to the total mean quartz contents. Abbreviations: Qtz = quartz; Ms = muscovite; Ill = illlite; Chl = chlorite; Kln = kaolinite; Pl = plagioclases; Ab = albite; KFs = K-feldspars. Conversion scaled weights: ****= 3.0 (very abundant) ***= 1.0 (abundant) **= 0.4-0.6 (frequent) *= 0.3-0.2 (present) tr <0.2 (traces) and – = not identified.

Profile site	Sample	Qtz	Ms	Ill	Chl	Kln	Pl	KFs
SP-1	R1	**	***	***	–	**	–	–
SP-2	R2	**	***		**	–	***	–
SP-3	R3	**	***		**	*	*	–
SP-4	R4	***	**		*	-	**	–
SP-5	R5	**	***		**	*	*	–
SP-6	R6	****	tr		–	–	tr	tr

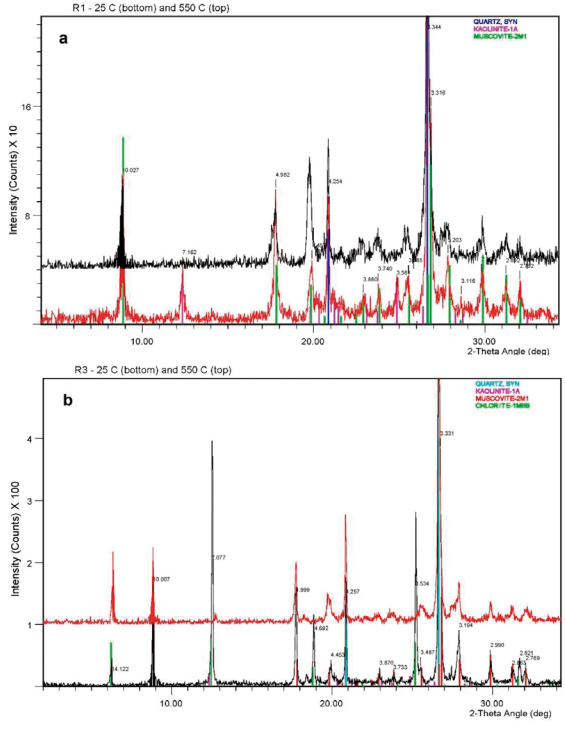

Figure 3. Rock powder unoriented XRD pattern, air-dried and solvated at room temperature 25 C (bottom line) and heated at 550 C (top line). Major minerals identified in a) sample R1 and b) sample R3. Only the range from 5° to 35°- 2θ is shown in the pattern.

The principal mineral phases present in the soil samples from the clay oriented aggregates patterns are given below in Table 3. In particular, the sequences are essentially the same identified before (micaceous phases and illite, with iron rich chlorite, traces of quartz, feldspars and minor kaolinite with some accompanying iron oxides). Particularly, only minor ferric amorphous species like lepidocrocite and iron oxides were identified as traces (Figure 4a). A Small peak at 6.2 Å on glycol (and also air-dried diffractogram) that disappears

on heating suggests a trace of iron oxides corresponding to lepidocrocite in S5 and S1 (Figure 4a). The presence of ferroan chlorite has been confirmed in samples S2.1, S2.2, S3.1, S3.2 (Figure 4b) and S5 through the strong peaks at 7.1 Å and 3.53 Å, with smaller peaks at 14 Å and 4.7 Å, suggesting an iron rich variety. Small peak at 3.58 Å on saturated patterns indicates additional minor kaolinite detected in samples S3.1, S3.2 (Figure 4b), S4 and S5. Peak at 7.1 Å, not significantly affected by heating accompanied by a small peak at 3.58 Å, especially on heating, suggests that kaolinite is also present (Figure 3a). The absence of strong peaks at 14 Å, 7.1 Å and 3.53 Å, especially with glycol, indicate that chlorite is not present in this particular sample (Figure 4a). Moreover, in the samples from S2 to S5 peaks at 14 Å, 7.1 Å and 3.53 Å, glycol solvated (Figure 4b), indicate presence of chlorite; a small peak at 3.58 Å on heating, suggests that kaolinite is also present (Figure 4b). Quartz (peaks at 3.35 and 4.26 Å) and K-feldspar (peak at 3.2 Å) are also representative in the composition of the soil samples showing sharp peaks in reflections (Figure 4b).

Table 3. Total chemical composition determined in the six profiles for parent rocks and soil samples. Contents of major components analysed by XRF and ICP-MS (weight %), *LOI (Loss On Ignition).

Profile site	Sample	Depth (cm)	SiO_2	Al_2O_3	Fe_2O_3	K_2O	MgO	CaO	Na_2O	TiO_2	P_2O_5	MnO	LOI*	Total
SP-1	R1	+18	56.67	23.38	5.79	4.89	0.73	0.26	0.50	1.00	0.06	0.02	6.74	100.04
	S1	0-18	67.01	17.58	7.31	3.85	0.63	0.41	0.48	0.79	0.16	0.02	1.15	99.39
SP-2	R2	+ 25	66.99	15.69	5.42	2.45	1.93	0.42	2.17	0.99	0.02	0.05	4.36	100.49
	S2.1	0-8	73.23	13.38	5.75	2.58	1.35	0.47	0.84	1.62	0.08	0.04	0.85	100.19
	S2.2	8-25	68.46	15.30	6.40	2.98	1.64	0.42	0.88	2.09	0.08	0.04	1.11	99.40
SP-3	R3	+ 20	59.69	20.03	6.64	3.13	1.69	0.52	1.42	1.10	0.07	0.07	5.68	100.04
	S3.1	0-12	63.84	19.85	7.91	2.97	1.35	0.35	0.80	1.14	0.12	0.04	1.04	99.41
	S3.2	12-20	65.22	19.82	7.50	2.15	1.53	0.34	0.70	1.24	0.10	0.05	0.76	99.41
SP-4	R4	+25	65.14	18.17	3.86	3.40	1.50	0.34	0.91	1.09	0.06	0.03	5.63	100.13
	S4	0-25	82.11	9.92	3.04	1.73	0.49	0.23	0.34	0.54	0.06	0.01	0.94	99.41
SP-5	R5	+15	56.80	22.72	7.63	2.95	1.77	0.46	0.93	1.13	0.08	0.07	5.84	100.38
	S5	0-15	60.80	22.11	9.30	1.94	1.06	0.32	0.86	1.61	0.15	0.17	1.07	99.39
SP-6	R6	+15	97.45	1.07	0.17	0.44	0.05	0.42	0.00	0.08	0.02	0.00	1.01	100.71
	S6	0-15	95.03	1.63	0.59	0.55	0.06	0.19	0.05	0.45	0.01	0.00	1.42	99.98

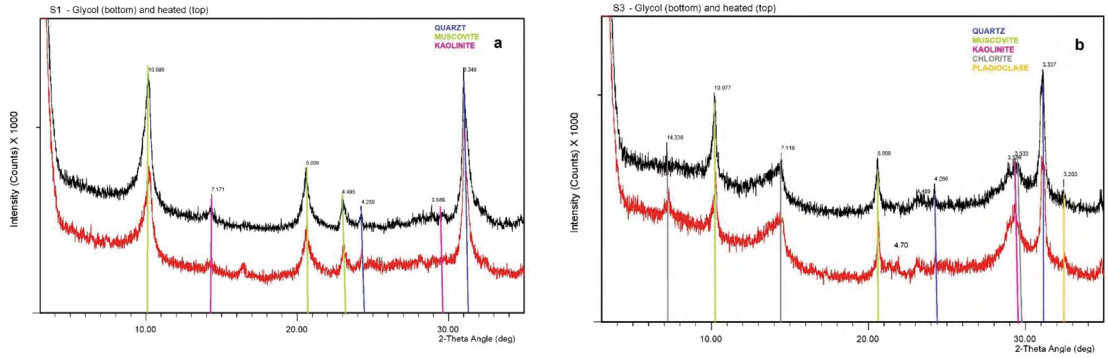

Figure 4. Clay oriented aggregates a XRD pattern from a representative sample a) S1 in the profile SP-1 and b) S3 in the profile SP-3 showing K-glycol treatment (bottom line) and heated at 400 C (top line). Only the range from 5° to 35°- 2θ is shown to clarify the interpretation in the pattern.

Rocks and soils geochemistry

The contents of major elements in the samples are summarized in Table 3. The contents found in the soils are coherent with those ones present in the rocks through the soil weathering profiles. SiO_2, Fe_2O_3 and Al_2O_3 contents are quite similar in soil profiles SP1 to SP5 being the most abundant elements. However in S6 from SP-6 the content of SiO_2 reaches about 95%, while in the rest of soil samples get around 65-70%. The bases K_2O, MgO, Na_2O and CaO are generally lower than those present in the rocks. K_2O (2-3%) shows higher contents among the last ones and, together with MgO (1-2%), are more abundant than CaO (0.2-0.4%) and Na_2O (0.5-0.9%). The content of Na_2O is slightly higher in the soil samples of SP-2 and SP-3 (Table 3). Regarding LOI results, the highest values correspond to SP-1 where R1 reaches 6.74 in the carboniferous series and the lowest to SP-6, where R6 is 1.01 (Table 3). The edaphic contents are little higher than the lithogenic ones for SiO_2, Fe_2O_3 and Al_2O_3 (Table 3). The parent rocks show relatively important amounts of Na_2O, Fe_2O_3 and MgO as well as K_2O which are retained in the less altered minerals (Table 3). So, the contents found in the residual soils show an enrichment of SiO_2, Fe_2O_3 and Al_2O_3 too (Table 3).

Chemical indices of alteration and element ratios

Weathering indices were calculated using molar proportions, increasing alteration indicated by increasing CIA (Chemical Index of Alteration; Nesbitt and Young, 1982), CIW (Chemical Index of Weathering; Harnois, 1988) and PIA (Plagioclase Index of Alteration; Fedo et al., 1995). CIW, CIA and PIA have reached higher values in SP-1, SP-3 and SP-5, all are in consonance with the geochemical base mobilization and depletion of major cations calculated (Table 4). However, minor differences have been shown in the present data from the soils and underlying rocks (Table 4). CIW and PIA show quite good correlation fitting (R^2=0.49) (Figure 5a), although CIA and PIA reaches a better correlation R^2=0.94. The fitting between CIW and CIA reaches a positive R^2=0.99. The higher values of the CIA and CIW are indicating a possible high grade of alteration, mainly in the rock samples from profiles SP-1, SP-3 and SP-5. PIW present high values specifically suggesting one of the most possible ways of primary mineral alteration (Table 4). It is also assumed that LOI, the only one not expressed as a ratio, increases with the degree of weathering. LOI has also resulted higher in SP-1, which is in consonance with the rest of indices calculated. A R^2=0.30 fitting in the correlation with CIW (Figure 5b) showing higher correlation in the rock series than the soil ones.

Table 4. Indices associated to the intensity of mineral alteration and weathering. Abbreviations: CIA: Chemical Index of Alteration; CIW: Chemical Index of Weathering; PIA: Plagioclase Alteration Index; Compositional molar ratios calculated from major oxides related to chemical and mineral weathering indices. Abbreviations: R_2O_3=(Fe_2O_3+Al_2O3); BxO=(Na_2O+K_2O+CaO+MgO).

Profile	Sample	Depth (cm)	CIA	CIW	PIA	SiO_2/ Al_2O_3	SiO_2/ R_2O_3	SiO_2/ TiO_2	SiO_2/ K_2O	BxO/ R_2O_3	BxO/ Al_2O_3	K_2O/ Na_2O	Al_2O_3/ Na_2O
SP-1	R1	+18	77.99	94.71	93.27	4.11	3.55	75.03	18.13	0.31	0.76	6.39	28.22
	S1	0-18	75.50	91.96	89.71	6.46	5.10	111.98	27.23	0.33	0.42	5.29	22.31
SP-2	R2	+ 25	69.20	78.36	75.06	7.23	5.92	89.55	42.81	0.62	0.55	0.74	4.40
	S2.1	0-8	72.68	85.65	82.54	9.27	7.28	59.80	44.48	0.50	0.63	2.01	9.64
	S2.2	8-25	73.79	87.40	84.55	7.58	5.98	43.45	35.90	0.49	0.63	2.24	10.61
SP-3	R3	+ 20	75.01	85.91	83.52	5.05	4.17	71.88	29.82	0.45	0.53	1.45	8.54
	S3.1	0-12	79.34	91.03	89.48	5.45	4.34	74.48	33.64	0.34	0.43	2.45	15.13
	S3.2	12-20	82.91	91.85	90.86	5.57	4.49	69.50	47.51	0.32	0.40	2.03	17.27
SP-4	R4	+25	75.79	89.53	87.22	6.07	5.35	79.43	29.99	0.46	0.44	2.46	12.13
	S4	0-25	77.67	90.99	89.12	14.01	11.72	201.79	74.41	0.35	0.41	3.33	19.37
SP-5	R5	+15	80.32	90.53	89.15	4.23	3.49	66.40	30.17	0.36	1.27	2.07	14.75
	S5	0-15	84.35	91.69	90.90	4.66	3.67	50.20	49.09	0.24	0.31	1.48	17.70
SP-6	R6	+15	46.18	58.14	43.50	154.21	139.73	1546.77	345.99	1.16	0.72	0.00	0.00
	S6	0-15	61.49	49.44	70.96	98.47	79.99	282.97	268.03	0.59	0.36	7.12	15.60

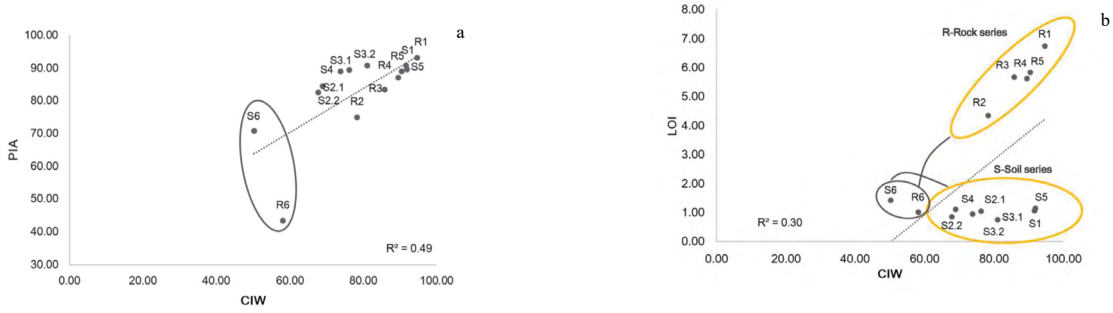

Figure 5. Correlation between chemical indices a) PIA and CIA b) LOI and CIW

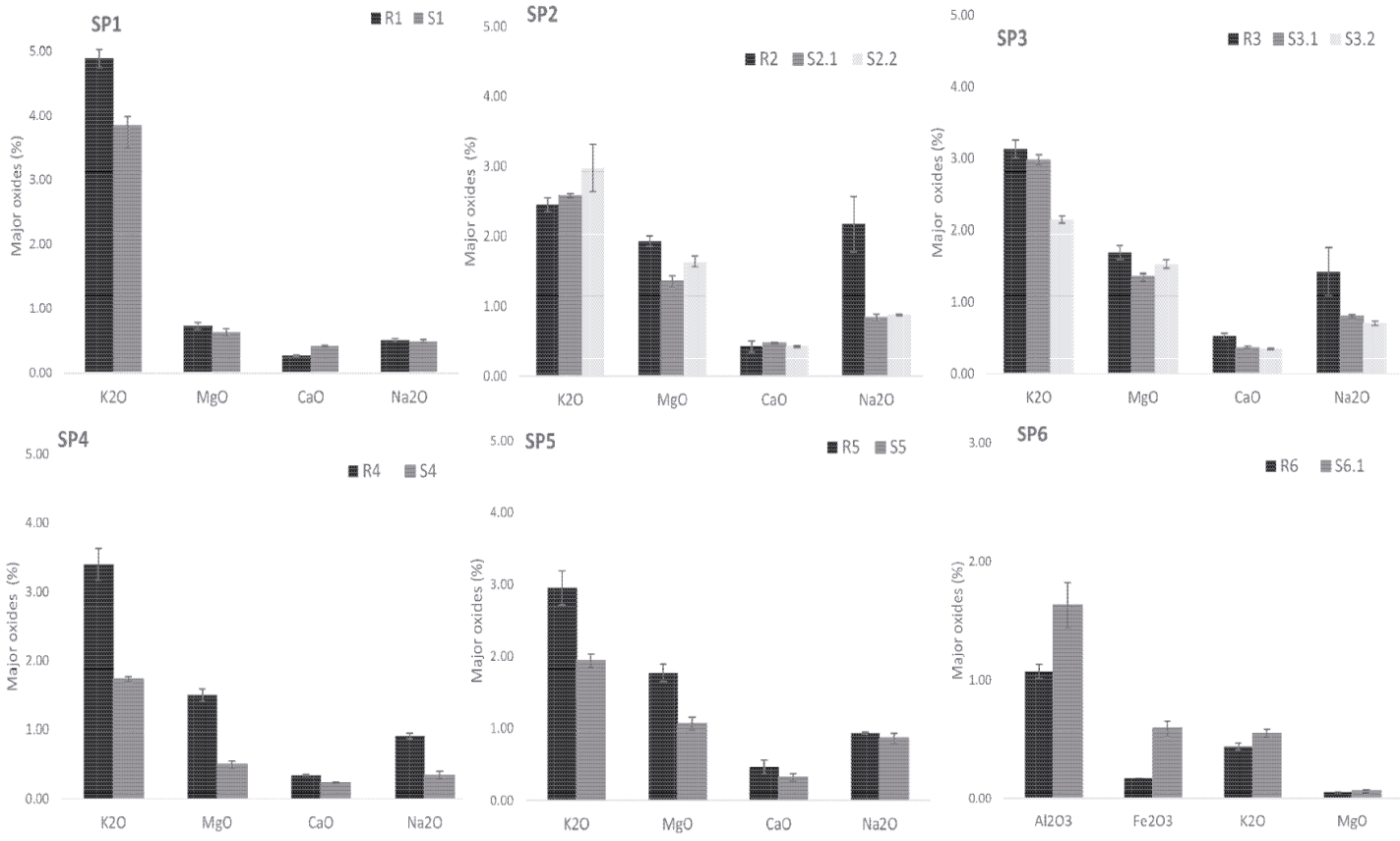

Figure 6. Enrichment and depletion in the soil profiles: composition of soil horizons showing mean concentrations and standard deviation of major components e xpressed in oxides (%).

Selected molar ratios, based on the principle that the ratio between concentrations of mobile (such as SiO_2, CaO, MgO, K_2O and Na_2O) and immobile elements (Al_2O_3, Fe_2O_3, TiO_2), should increase with weathering have been studied. These molar ratios such as SiO_2/Al_2O_3 (Table 4) related to silica leaching result a dominant factor in the characterization of the weathering together with Chemical Weathering Indices (CIW, CIA and PIA) related to weathering intensity. The main chemical indices are expected to increase over time as leaching progresses. Some other selected ratios form the literature present a different behavior. For instance, SiO_2/K_2O tends to show lower values when the weathering is higher (SP-1) (Table 4). Opposite to that, SiO_2/TiO_2 remains almost constant with no noticeable differences as well as SiO_2/Al_2O_3 and SiO_2/R_2O_3 both are in consonance among the rocks and soil samples not showing remarkable differences (Table 4). Other ratios regarding the bases give an estimation of weatherable primary minerals remaining in soils, such as BxO/R_2O_3 and BxO/Al_2O_3 (Table 4), decreases over time, so less weathered materials, for instance R6, present higher values (Table 4). K_2O/Na_2O and $Al_2O_3/Na2O$ are both good indicators the weathering degree showing lower values related to less alteration (SP-2) and higher values for more altered phases (SP-1) (Table 4).

Discussion

Geochemical relations, elements mobility and mineral alteration

In general, the relative chemical composition variations are neither high nor too significant, comparing the upper and lower parts in the profiles, since the sampling depth is rather limited (Table 3). Generally, the profiles present an increasing content of some elements, noticeable in SiO_2, Al_2O3, and Fe_2O_3, from the parent rocks to the upper levels of the soil profiles (Table 3) while cations are leached. It is particularly important the relatively high K_2O content found in all of soils, especially in SP-1 (Figure 6). Na_2O, MgO and CaO are present in soils, but not significantly enriched (Figure 6). According to the results, there is a net gain of SiO_2, Al_2O_3, and Fe_2O_3 in the soils, in particular, from profiles SP-1, SP-3 and SP-5 (Table 3). Otherwise, K_2O, MgO, CaO and Na_2O are still relatively higher in the parent rocks (Figure 6), this last one especially in sample R2 from SP-2 due to the abundance of albite (Table 2). However, other leachable elements such as CaO do not show this clear tendency, so the content is rather limited in both rocks and soils, since it is only enriched in SP-1 (Figure 6). Meanwhile, soil MgO gain seems to be more evident, in lower parts of SP-2 and SP-3 (Figure 6) but limited in the rest. The K_2O depletion from rocks and enrichment in soils, particularly shown in SP-1 and SP-6, is mainly the result of micas alteration (Figure 6).

The bases mobilities against iron sesquioxides are evident, but not high. The alteration causes hardly any variation in the relative amounts of Na_2O and MgO, but leaching in the upper layers preferentially eliminates MgO (Figure 6). Exactly the same happens with CaO with respect to Na_2O. The mobility of K_2O is always greater than Na_2O, and K_2O, seems to be the most mobile, as there may be no minerals to retain it. In short, a gradual depletion of bases and enrichment in SiO_2 and iron and aluminium sesquioxides is observed. Al_2O_3 contents found in soils are not higher than those ones in rocks (Figure 6). Al_2O_3 is slightly less common in soils, particularly in SP-4 and SP-1 and less noticeable in the rest (Figure 6). Indeed, the enrichment of silica, though not marked, is observed in most of soil profiles, especially in SP-4. SiO_2 accumulation is normally followed by SiO_2 mobilization and partial desilification, according to the removal as soluble colloidal form leached out of the profile. Under these climatological conditions the intense leaching left a material poor in bases, since there is hardly any variation in their content.

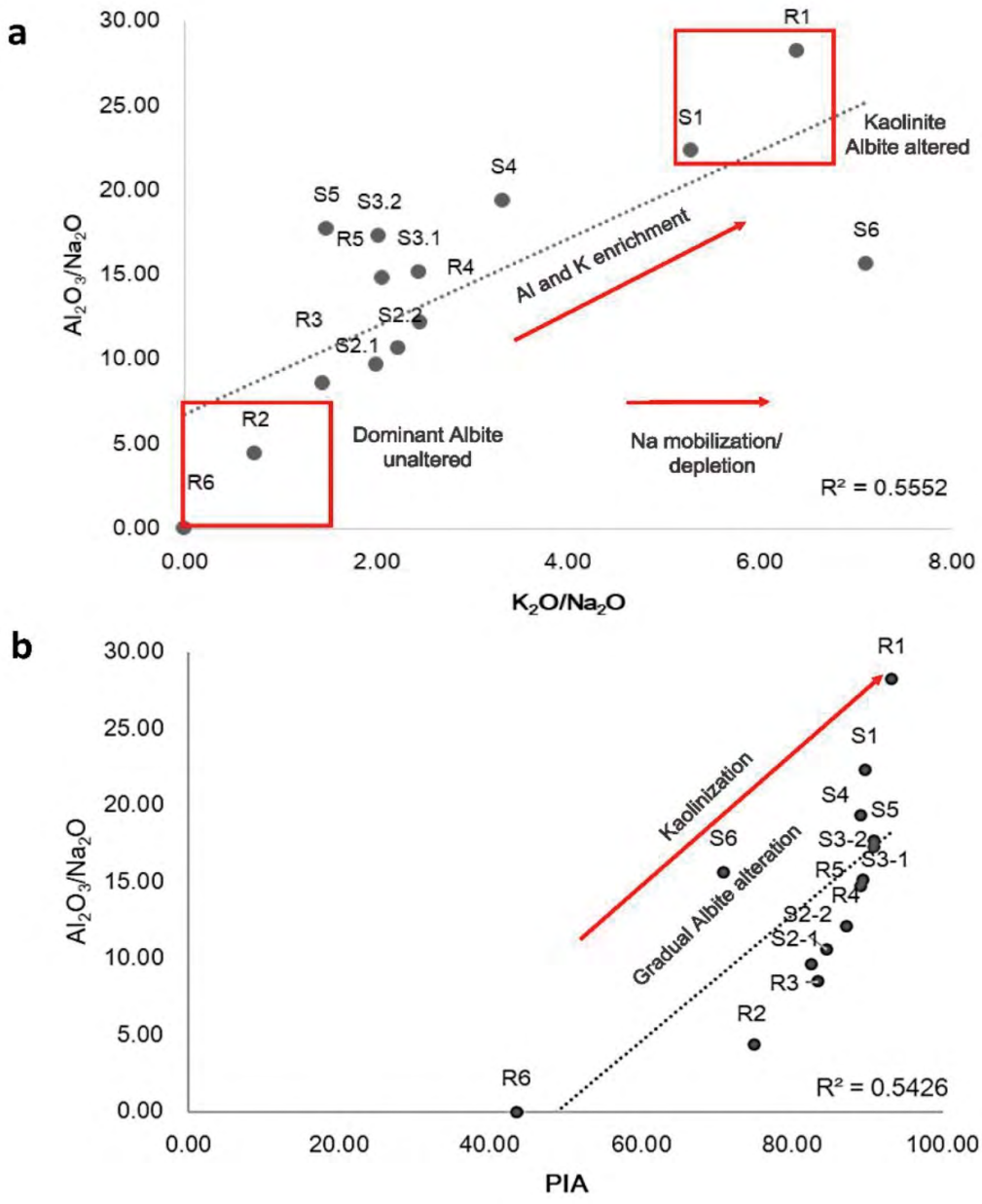

Figure 7. Cross data plots within linear correlation and R2 fitting for a) Al_2O_3/Na_2O and K_2O/Na_2O and b) Al_2O_3/Na_2O and PIA

Lower Al_2O3 found in soils than in underlying rocks must be related with other physical processes besides chemical decomposition related to the removal of fine-grained clay particles enriched in Al_2O_3. Dinis & Oliveira (2016) explained that the composition of metasedimentary-derived sediments is not substantially affected by their grain size distributions. It could be explained by the dissolution leaching out of the profile, as colloidal particles clay fractions enriched in Al_2O_3, as happens when SiO_2 migrates in the edaphic environment. This could explain the lower Al_2O_3 contents found in some soils due to dissolution, leaching and final depletion out from the soil profile.

As seen before, the profiles experience a gradual and little noticeable mobilization of bases from the destruction of the dominant primary minerals, mainly micas, Fe-bearing chlorites and feldspars and plagioclases, which is followed by a depletion in the upper parts of the soil profiles as well, as seen in Doval et al. (2012), Ling et al. (2016) and (2018). These losses were particularly observed in the early stages of the soils pedological development in agreement with Senol et al. (2016). It is common generalizing the genesis of highly weathered soils which results in intense loss of bases (Na_2O, CaO, K_2O and MgO), whereas less soluble Al2O3 accumulates in newly formed solid phases such as secondary 1:1 phyllosilicates like kaolinite, or mineral forms of aluminium hydroxide, such as gibbsite too (Romero et al. 1992). However, Taboada & García (1999) showed that much evolution of the material is not necessary to explain the abundance of kaolin minerals and gibbsite, as these are compatible in many saprolites with absolutely fresh feldspars; in this case explaining the coexistence of albite and kaolinite supporting the evidence shown in this paper. Taboada & Garcia (1999) also reported that gibbsite may even be the mineralogical product formed from the plagioclases in the initial weathering stages when intense leaching occurs.

Albite alteration supported by chemical indices

Indices associated to the intensity of mineral alteration and chemical weathering (CIW, CIA and PIA) give a quantitative measure of feldspar weathering, by relating Al_2O_3 enrichment in the weathering in contrast to Na_2O, CaO and K_2O, which should be removed from the soil profile during plagioclase or K-feldspar weathering (Nesbitt and Young, 1982; White et al., 2001; Price and Velbel, 2003). Some element ratios biplots shown in Figure 7, help to clarify the interpretation. The molar ratios Al_2O_3/Na_2O and K_2O/Na2O (Figure 7a) show clearly differences, mainly in SP-2 sample R2 where albite composition is higher and the ratios for mobile/mobile elements K_2O/Na_2O and Al_2O_3/Na_2O (Figure 7a) show the opposite in SP-1 where kaolinite is dominant in composition, due to in R1 and S1 albite is not present. Al_2O_3/Na_2O with K_2O/CaO with a correlation fit R2=0.56, indicative of the possible weathering increase with a linear positive tendency of the plot (Figure 7a). Al_2O_3 and K_2O enrichment and Na_2O mobilization are both indicative of the gradual plagioclase alteration, so chemical indices support the main hypothesis in this case of albite alteration. The cross-dot plots reflect a good fitting and indicate mineral composition, where albite unaltered is dominant or kaolinite is dominant (Figure 7a). Furthermore, Al_2O_3/Na_2O result a key factor in the characterization of the grade of weathering (Figure 7b), when plotting against Plagioclase Index of Alteration (PIA) (Fedo et al., 1995) and with Chemical Weathering Indices (CIW) (Harnois, 1988). Al2O3/Na2O is considered a good indicator of the degree of weathering if we supposed lower values for less altered materials where plagioclases (albite) still remain in parent rocks. Weathering chemical indices selected PIA and CIW show a clear correlation, similar to the one obtained for Al_2O_3/Na_2O and PIA for rock and soil series (Figure 7b). This positive correlation (R2=0.54) indicates a progressive weathering of albite while advancing the kaolinization in the most altered soil profiles SP-1, as the higher PIA values suggest, and less alteration in SP-2 (Figure 7b). In short, cations such as Na, K and Ca commonly generated by the weathering of feldspar and plagioclases into kaolinite, are rapidly release in the soil domain (Fedo et al., 1995). PIA, CIW and CIA and other chemical relations such as Al_2O_3/Na_2O help to understand the most reliable assumption that kaolinite comes from the gradual alteration of albite. Despite the evidence of element leaching, although quite limited, during the data evaluation, geochemical indices such as PIA and Al_2O_3/Na_2O ratio are good indicators of possible differential weathering intensities in these profiles.

Differential weathering signatures

The main findings point out some possible differential weathering signatures supporting the mineral alteration of albite, especially the clue given by the identification of primary phyllosilicates and their coexistence with other secondary phases. This finding gives some enlightening data indicative of possible different processes affecting the alteration profiles. Particularly, special emphasis is given to the albite occurrence, which is found coexisting with kaolinite in the mineral sequences found in the profiles. This assumption may be explained by at least three particular conditions as shown in literature. Kaolinite, firstly supposed to be directly inherited in soils from the parent substrates when formerly present (especially abundant in R1 from SP-1). However, this explanation was not enough in the profiles where kaolinite does not exist originally since the edaphic formation of this mineral from the weathering of silicates requires extreme alteration condition (Molina et al., 1990; Hernando Massanet et al., 2004); not possible in the current studied soil conditions. Secondly, the weathered plagioclases drive to the occurrence of derived secondary kaolinite associated to a pedogenic origin (Driese et al., 2007; Churchman & Lowe, 2012). Strong pedogenic dissolution and alteration of feldspars and mafic minerals to kaolinite, gibbsite and iron oxides, as well as geochemical losses of Na, Ca, Mg and K (Driese et al., 2007) must be necessary to understand this fact occurring under particular conditions. In this work, the results have shown certain amounts of amorphous species like lepidocrocite and other iron oxides which are also associated to organic phases and weathering process in slates and shales rich in sulphides and organic phases, which are the dominant parent rocks. Adding to the previous, the hydrolytic weathering the main cause of a progressive transformation of affected components into clay minerals, ultimately into kaolinite (Romero et al. 1992; Taboada & García, 1999), following the silicate weathering generally known as monosialitization. This acid hydrolysis favors the mobilizations of some bases, including in later stages, and the release of Ba and K from the partial alteration of K-feldspars, plagioclases and micas (Fernández-Caliani & Cantano, 2010). In short, kaolinite has been widely shown as the stable weathering product of the feldspars, plagioclases (albite) and muscovite (Núñez & Recio, 2007). In such context, it could enhance to explain, at least partially, the formation of secondary clay minerals belonging to the kaolinite group and the expansive clays and 2:1 mixed layers, more abundant in areas where a dry period of intense evaporation generally occurs.

Finally, the last assumption may explain that kaolinite and albite could coexist in different size-fractions because weathering was still not able to destroy all albite. These rock substrates which are mainly made up of fine to very fine fractions, mainly silt and clay particles, are not supposed to be substantially affected by the grain size distribution of the sediment in agreement with Dinis & Oliveira (2016). Moreover, very fine grained fractions in the profiles may be depleted due to loss process controlled by diverse physical factors driven by topography (Tardy et al., 1973), remaining in the soils only the coarser fractions. This is directly linked to mechanical weathering and erosion rates. This last explanation associated to intense erosive activity requires great mineral similarity among weathered and fresh substrates, together with a low development in the soil profiles due to a continuous renovation-denudation in the recycling.

No less important is the narrow relationship which links geochemical composition with the contrasting climatic conditions. Dinis et al. (2020) and Perri (2020) have recently showed how chemical indices act as good proxies for chemical weathering to reconstruct past climate conditions. Dinis et al. (2016 and 2017) have also investigated the roles played by distinct processes on the weathering intensity and the palaeoclimatic conditions, demonstrating the composition of clay is strongly influenced by climatically driven weathering. Otherwise, Perri (2018) has shown higher abundance of kaolinite related to warm–humid conditions. Moreover, Perri (2020) released medium-low CIA values for similar climatic areas, in terms of mean annual temperature and precipitation, which underwent moderate-weak chemical weathering similar to this study. The results do not differ a lot from the values found in this study for the CIW, CIA and PIA; quite similar too to those obtained in previous works of Scarciglia et al. (2016) or Perri (2016).

In the light of the chemical indices and the linkages showing good relations with geochemical data, in this particular case, the albite hydrolytic alteration weathering by acid dissolution is still the main hypothesis supporting the presence of kaolinite in the most altered investigated soil profiles. Perri et al. (2015) demonstrated in granitoid weathering simulations the CO2-controlled dissolution of albite-rich plagioclase is the most important reaction, followed by the dissolution of K-feldspar, biotite, chlorite, and muscovite, in order of decreasing importance. In fact, differential chemical weathering occurring in the acidic solution of soils seems to better explain this way of alteration. The acidic solution from the oxidation of both, organic matter, quite important in the composition, and sulphides, abundant in the rocks, could explain the ways of alteration, supporting the presence of such abundant kaolinite. Some authors have already demonstrated the influence of organic matter in the acid dissolution to explain kaolinite presence (Gallardo Lancho et al.1976; Romero et al. 1992, Fischer et al., 2009; Li et al., 2014; Emberson et al., 2016; Ling et al., 2016). Solute transfer and elements mobility by acidic percolation of soil solutions should be studied further in order to clarify this assumption. So that, solute transfer and elements mobility by acidic percolation of soil solutions and leaching data should be studied further to give a concluding explanation like in other studies supported by Cronan (1985), Bain (2007) or Di Figlia, et al. (2007).

Conclusions

The identification of primary phyllosilicates and their coexistence with other secondary clays gives an enlighten clue indicative of possible different

weathering processes affecting the soil profiles. Particularly, special emphasis is given to the albite occurrence, which is found coexisting with kaolinite in most of the mineral sequences. Kaolinite can be directly inherited in soils from parent rocks and partially due to mineral alteration, preferably from albite. In addition, since both could coexist in different size-fractions they are differently affected by weathering. So, it may be concluded that the geochemical composition must be also substantially affected by the grain size distribution of the sediment. Moreover, good correlations between chemical indices and element ratios, may indicate kaolinite in this case should come from the alteration of plagioclases during weathering.

The traditional chemical indices have also helped to understand different chemical weathering processes taking place. PIA, CIW and CIA have resulted an essential tool to infer some assessment due to the lack of other more specific data; giving a measure of plagioclase differential weathering; they together with, Al_2O_3/Na_2O and K_2O/Na_2O, have also supported that kaolinite comes from the gradual alteration of albite mainly due to acid hydrolysis.

The differential weathering and albite alteration detected in these profiles is in agreement with the mobility of major elements leading to a general loss of bases (Na_2O, CaO, K_2O and MgO). In this work, the relations between the parent rocks composition and soils can easily assist in determining the bases loss and the K_2O enrichment from the bottom to upper parts in the soil profiles. In general, a slight enrichment in silica and iron and aluminium sesquioxides attributed to the advancing process of weathering in agreement with most of findings show. However, Al_2O_3 in some profiles is slightly less abundant in soils than in parent rocks, probably because Al_2O_3 in the finest clay fractions is being lost by physical processes. Similarly occurring with SiO_2, firstly enriched in the soil profiles when weathering advances and, later, leached out of the profile. Hence, besides chemical weathering, other physical or mechanical processes, due to erosion and removal, are expected to take placein such favorable topographic conditions. This together with a low development detected in the soil profiles leads to think of a continuous renovation-denudation in the recycling. In short, several factors, not only data limited to geological source areas and the critical lithology control, mainly based on geochemical and mineralogical composition, but also morphology and topography, climatic registers, or even vegetation interactions, may be assessed on weathering research.

Acknowledgments

The authors want to express their gratitude to the Editors, Editor-in-Chief and the anonymous reviewers for their exhaustive reviews and valuable suggestions on the manuscript which helped to enrich the scientific discussion. Thanks for the support given by Dr. Fernando Gómez-Fernández on the performance of SEM analysis and especially for his expertise on mineralogy interpretations. The authors would also like to thank the help given with the XRD analysis by the School of Biological, Earth and Environmental Sciences University of New South Wales (UNSW). We are also grateful for the help provided by the microscopy laboratory service (University of León, Spain). The assistance and the technical support provided by the Structural Analysis Unit SAI-UAE (University of Coruña, Spain) and the Technical Scientific Services (University of Oviedo, Spain). This research was funded by the Educational and Research authority from Castilla & León Regional Government (LEOO3A08) and supported by the Spanish Ministry of Education and Science (EDU/1262/2009), first author's PhD funding project.

References

Anderson, D. H. & Hawkes, H. E. (1958). Relative mobility of the common elements in weathering of some schist and granite areas. *Geochimica et Cosmochimica Acta*, 14(3), 204-210. https://doi.org/10.1016/0016-7037(58)90079-6

Anderson, S. P., Dietrich, W. E. & Brimhall Jr, G. H. (2002). Weathering profiles, mass-balance analysis, and rates of solute loss: Linkages between weathering and erosion in a small, steep catchment. *Geological Society of America Bulletin*, 114(9), 1143-1158. https://doi.org/10.1130/0016-7606(2002)114<1143:WPMBAA>2.0.CO;2

Aspandiar, M. F. & Eggleton, R. A. (2002). Weathering of chlorite: I. Reactions and products in microsystems controlled by the primary mineral. *Clays and Clay Minerals,* 50(6), 685-698. https://doi.org/10.1346/000986002762090227

Bain, D. C., Mellor, A. & Wilson, M. J. (1990). Nature and origin of an aluminous vermiculitic weathering product in acid soils from upland catchments in Scotland. *Clay Minerals,* 25(4), 467-475. https://doi.org/10.1180/claymin.1990.025.4.05

Bain, D.C. (2007). *Soil clay minerals and their relevance to environmental change*. Macla, 7, 57-59.

Banfield, J. F. & Eggleton, R. A. (1990). Analytical transmission electron microscope studies of plagioclase, muscovite, and K-feldspar weathering. *Clays and Clay Minerals,* 38(1), 77-89. https://doi.org/10.1346/CCMN.1990.0380111

Barba, P., Nozal, F., Rodríguez, A. S. & Suárez, A. (1994). *II: Estratigrafía*. In: ITGE (editor). Mapa Geológico de la Provincia de León a escala 1:200000. Instituto Tecnológico Geominero de España, Diputación de León, 13-90.

Chesworth, W. (1973a). The parent rock effect in the genesis of soil. *Geoderma*, 10 (3), 215-225. https://doi.org/10.1016/0016-7061(73)90064-5

Chesworth, W. (1973b). The residua system of chemical weathering: a model for the chemical breakdown of silicate rocks at the surface of the earth. *Journal of Soil Science,* 24 (1), 69-81. https://doi.org/10.1111/j.1365-2389.1973.tb00742.x

Churchman, G. J. & Lowe, D. J. (2012). *Alteration, formation, and occurrence of minerals in soils*. In: Huang, P. M.; Li, Y. & Sumner, M. E. (Editors). Handbook of Soil Sciences. 2nd edition. Vol. 1: Properties and Processes. CRC Press (Taylor& Francis), Boca Raton, FL, 20, 1-20. 72 pp. https://hdl.handle.net/10289/9024

Colmenero, J. R., Fernández, L. P., Moreno, C., Bahamonde, J. R., Barba, P., Heredia, N., et al. (2002). *Carboniferous*. In: Gibbons, W. & Moreno, T. (Editors). Geology of Spain. London, The Geological Society of London, 120–153.

Cronan, C. S. (1985). *Chemical weathering and solution chemistry in acid forest soils: differential influence of soil type, biotic processes, and H+ deposition.* In: The chemistry of weathering. Springer, Dordrecht, 175-195. https://doi.org/10.1007/978-94-009-5333-8_11

Di Figlia, M. G., Bellanca, A., Neri, R. & Stefansson, A. (2007). Chemical weathering of volcanic rocks at the island of Pantelleria, Italy: Information from soil profile and soil solution investigations. *Chemical Geology*, 246 (1-2), 1-18. https://doi.org/10.1016/j.chemgeo.2007.07.025

Dinis, P. & Oliveira, Á. (2016). Provenance of Pliocene clay deposits from the Iberian Atlantic Margin and compositional changes during recycling. *Sedimentary Geology*, 336, 171-182. https://doi.org/10.1016/j.sedgeo.2015.12.011

Dinis, P. A., Dinis, J. L., Mendes, M. M., Rey, J. & Pais, J. (2016). Geochemistry and mineralogy of the Lower Cretaceous of the Lusitanian Basin (western Portugal): Deciphering palaeoclimates from weathering indices and integrated vegetational data. *Comptes Rendus Geoscience*, 348(2), 139-149. https://doi.org/10.1016/j.crte.2015.09.003

Dinis, P., Garzanti, E., Vermeesch, P. & Huvi, J. (2017). Climatic zonation and weathering control on sediment composition (Angola). *Chemical Geology,* 467, 110–121. https://doi.org/10.1016/j.chemgeo.2017.07.030

Dinis, P. A., Garzanti, E., Hahn, A., Vermeesch, P. & Cabral-Pinto, M. (2020). Weathering indices as climate proxies. A step forward based on Congo

and SW African river muds. *Earth-Science Reviews*, 201, 103039. https://doi.org/10.1016/j.earscirev.2019.103039

Doval, M., Martín-García, R., La Iglesia, Á. & Alonso-Zarza, A. M. (2012). Clay minerals associations in palaeoweathering profiles from Central Spain: genesis and implications. *Clay Minerals,* 47(1), 117-129. https://doi.org/10.1180/claymin.2012.047.1.117

Driese, S. G., Medaris Jr, L. G., Ren, M., Runkel, A. C. & Langford, R. P. (2007). Differentiating pedogenesis from diagenesis in early terrestrial paleoweathering surfaces formed on granitic composition parent materials. *The Journal of Geology*, 115(4), 387-406. https://doi.org/10.1086/518048

Eberl, D. D., Farmer, V. C. & Barrer, R. M. (1984). Clay mineral formation and transformation in rocks and soils. *Philosophical Transactions of the Royal Society of London A: Mathematical, Physical and Engineering Sciences*, 311 (1517), 241-257. https://doi.org/10.1098/rsta.1984.0026

Emberson, R., Hovius, N., Galy, A. & Marc, O. (2016). Oxidation of sulfides and rapid weathering in recent landslides. *Earth Surface Dynamics*, 4(3), 727-742. https://doi.org/10.5194/esurf-4-727-2016

Ezzaım, A., Turpault, M. P. & Ranger, J. (1999a). Quantification of weathering processes in an acid brown soil developed from tuff (Beaujolais, France): Part I. Formation of weathered rind. *Geoderma*, 87(3-4), 137-154. https://doi.org/10.1016/S0016-7061(98)00061-5

Ezzaım, A., Turpault, M. P. & Ranger, J. (1999b). Quantification of weathering processes in an acid brown soil developed from tuff (Beaujolais, France): Part II. Soil formation. *Geoderma*, 87 (3-4), 155-177. https://doi.org/10.1016/S0016-7061(98)00061-5

Fedo, C. M., Wayne Nesbitt, H. & Young, G. M. (1995). Unraveling the effects of potassium metasomatism in sedimentary rocks and paleosols, with implications for paleoweathering conditions and provenance. *Geology,* 23(10), 921-924. https://doi.org/10.1130/0091-7613(1995)023<0921:UTEOPM>2.3.CO;2

Fernández-Caliani, J. C. & Cantano, M. (2010). Intensive kaolinization during a lateritic weathering event in South-West Spain: mineralogical and geochemical inferences from a relict paleosol. *Catena*, 80 (1), 23-33. https://doi.org/10.1016/j.catena.2009.08.005

Fischer, C., Schmidt, C., Bauer, A., Gaupp, R. & Heide, K. (2009). Mineralogical and geochemical alteration of low-grade metamorphic black slates due to oxidative weathering. *Geochemistry,* 69 (2), 127-142. https://doi.org/10.1016/j.chemer.2009.02.002

Gallardo Lancho, J., Camazano, M.S., Alonso, J. S. & Sánchez, Y. G. (1976). Influencia de la materia orgánica en la génesis de gibsita y caolinita en suelos graníticos del centro-oeste de España. *Clay Minerals*, 11(3), 241-249. https://doi.org/10.1180/claymin.1976.011.3.06

Gardner, R. & Walsh, N. (1996). Chemical weathering of metamorphic rocks from low elevations in the southern Himalaya. *Chemical Geology*, 127(1-3), 161-176. https://doi.org/10.1016/0009-2541(95)00089-5

Guan, P., Ng, C. W. W., Sun, M. & Tang, W. (2001). Weathering indices for rhyolitic tuff and granite in Hong Kong. *Engineering Geology*, 59(1-2), 147-159. https://doi.org/10.1016/S0013-7952(00)00071-5

Harnois, L. (1988). The CIW index: a new chemical index of weathering. *Sedimentary geology*, 55, 319-322. https://doi.org/10.1016/0037-0738(88)90137-6

Harriss, R. C. & Adams, J. A. (1966). Geochemical and mineralogical studies on the weathering of granitic rocks. *American Journal of Science*, 264(2), 146-173. https://doi.org/10.2475/ajs.264.2.146

Hernando Massanet, M. I., Barba Carretero, A. M. & Hernando Costa, J. (2004). Mineralogía de suelos de la Sierra de Guadarrama (Madrid, España). *Cuaternario y Geomorfología,* 18(1-2), 67-71.

Jayawardena, U. D. S. & Izawa, E. (1994). A new chemical index of weathering for metamorphic silicate rocks in tropical regions: a study from Sri Lanka. *Engineering Geology*, 36(3-4), 303-310. https://doi.org/10.1016/0013-7952(94)90011-6

Jiménez-Espinosa, R., Vázquez, M. & Jiménez-Millán, J. (2007). Differential weathering of granitic stocks and landscape effects in a Mediterranean climate, Southern Iberian Massif (Spain). *Catena,* 70(2), 243-252. https://doi.org/10.1016/j.catena.2006.09.001

Johnson, N. M., Likens, G. E., Bormann, F. H. & Pierce, R. S. (1968). Rate of chemical weathering of silicate minerals in New Hampshire. *Geochimica et Cosmochimica Acta,* 32(5), 531-545. https://doi.org/10.1016/0016-7037(68)90044-6

Klug, H. P. & Alexander, L. E. (1974). *X-ray diffraction procedures: for polycrystalline and amorphous materials*. Second edition, Wiley-VCH, U.S.A., 992 pp.

Li, S. L., Chetelat, B., Yue, F., Zhao, Z. & Liu, C. Q. (2014). Chemical weathering processes in the Yalong River draining the eastern Tibetan Plateau, China. *Journal of Asian Earth Sciences,* 88, 74-84. https://doi.org/10.1016/j.jseaes.2014.03.011

Ling, S., Wu, X., Sun, C., Liao, X., Ren, Y. & Li, X. (2016). Mineralogy and geochemistry of three weathered Lower Cambrian black shale profiles in Northeast Chongqing, China. *Geosciences Journal*, 20 (6), 793-812. https://doi.org/10.1007/s12303-016-0008-y

Ling, S., Wu, X., Zhao, S. & Liao, X. (2018). Evolution of porosity and clay mineralogy associated with chemical weathering of black shale: a case study of Lower Cambrian black shale in Chongqing, China. *Journal of Geochemical Exploration,* 188, 326-339. https://doi.org/10.1016/j.gexplo.2018.02.002

Marcos, A., Martínez-Catalán, J. R., Pérez-Estaún, A., Pulgar, J. A. & Vera, J. A. (2004). *Características generales de la estructura de la Zona Asturoccidental-leonesa*. In: Vera, J. A. (Ed). Geología de España, SGE-IGME, Madrid, 54-55 pp.

Martínez-Catalán, J. R., Pérez-Estaún, A., Bastida, F., Pulgar, J. A. & Marcos, A. (1990) *West Asturian-Leonese Zone. Structure*. In: Dallmeyer, E. & Martínez-García (Eds.). Pre-Mesozoic Geology of Iberia, R.D., Springer-Verlag, Berlin, 103-114 pp.

Merriman, R. J., Roberts, B. & Peacor, D. R. (1990). A transmission electron microscope study of white mica crystallite size distribution in a mudstone to slate transitional sequence, North Wales, UK. *Contributions to Mineralogy and Petrology*, 106(1), 27-40. https://doi.org/10.1007/BF00306406

Meunier, A., Sardini, P., Robinet, J. C. & Prêt, D. (2007). The petrography of weathering processes: facts and outlooks. *Clay Minerals*, 42(4), 415-435. https://doi.org/10.1180/claymin.2007.042.4.01

Meunier, A., Caner, L., Hubert, F., El Albani, A. & Prêt, D. (2013). The weathering intensity scale (WIS): An alternative approach of the chemical index of alteration (CIA). *American Journal of Science,* 313(2), 113-143. https://doi.org/10.2475/02.2013.03

Molina, E., Cantano, M., Rodriguez, P. G. & Vicente, M. A. (1990). Some aspects of paleoweathering in the Iberian Hercynian Massif. *Catena*, 17(4-5), 333-346. https://doi.org/10.1016/0341-8162(90)90036-D

Molina, E., González, M. G. & Espejo, R. (1991). Study of paleoweathering on the Spanish Hercynian basement Montes de Toledo (central Spain). *Catena,* 18(3-4), 345-354. https://doi.org/10.1016/0341-8162(91)90030-2

Molina, E. & Cantano M. (2002). Study of weathering processes developed on old piedmont surfaces in Western Spain: new contributions to the interpre-

tation of the "Raña" profiles. *Geomorphology,* 42(3-4), 279-292. https://doi.org/10.1016/S0169-555X(01)00091-5

Moore, D. M. & Reynolds, R. C. (1989). *X-ray Diffraction and the Identification and Analysis of Clay Minerals* (Vol. 322). Oxford: Oxford University press, 321 pp.

Munroe, J. S., Farrugia, G. & Ryan, P. C. (2007). Parent material and chemical weathering in alpine soils on Mt. Mansfield, Vermont, USA. *Catena,* 70(1), 39-48. https://doi.org/10.1016/j.catena.2006.07.003

Nesbitt, H. W., Markovics, G. & Price R. C. (1980). Chemical processes affecting alkalis and alkaline earths during continental weathering. *Geochimica et Cosmochimica Acta,* 44(11), 1659-1666. https://doi.org/10.1016/0016-7037(80)90218-5

Nesbitt, H. W. & Young, G. M. (1982). Formation and diagenesis of weathering profiles. *The Journal of Geology*, 97(2), 129-147. https://doi.org/10.1086/629290

Núñez, M. A. & Recio, J. M. (2007). Kaolinitic paleosols in the southwest of the Iberian Peninsula (Sierra Morena region, Spain). Paleoenvironmental implications. *Catena,* 70(3), 388-395. https://doi.org/10.1016/j.catena.2006.11.004

Papoulis, D., Tsolis-Katagas, P. & Katagas, C. (2004). Progressive stages in the formation of kaolin minerals of different morphologies in the weathering of plagioclase. *Clays and Clay Minerals*, 52(3), 275-286. https://doi.org/10.1346/CCMN.2004.0520303

Parker, A. (1970). An index of weathering for silicate rocks. *Geological Magazine,* 107, 501–504. https://doi.org/10.1017/S0016756800058581

Pédro, G. (1997). Clay minerals in weathered rock materials and in soils. In: Soils and sediments. Springer, Berlin, Heidelberg, 1-18pp. https://doi.org/10.1007/978-3-642-60525-3_1

Pérez-Estaún, A., Bastida, F., Martínez-Catalán, J. R., Gutiérrez Marco, J. C., Marcos, A. & Pulgar, J. A. (1990). *The West Asturian-Leonese zone. Stratigraphy*. In: Dallmeyer, R. D. & Martínez-García, E. (Editors). Pre-Mesozoic Geology of Iberia, Springer-Verlag, Berlin, 92-102. https://doi.org/10.1007/978-3-642-83980-1_3

Pérez-Estaún, A., Bea, F., Bastida, F., Marcos, A., Martínez-Catalán, J. R., Arenas, R., Díaz García, F., Azor, A., Simancas, J. F. & González Lodeiro, F. (2004). *La Cordillera Varisca Europea: El Macizo Ibérico*. In: Vera, J. A. (Editor). Geología de España, SGE-IGME, Madrid, 17-25.

Perri, F. (2018). Reconstructing chemical weathering during the Lower Mesozoic in the Western-Central Mediterranean area: a review of geochemical proxies. *Geological Magazine*, 155(4), 944-954. https://doi.org/10.1017/S0016756816001205

Perri, F. (2020). Chemical weathering of crystalline rocks in contrasting climatic conditions using geochemical proxies: An overview. *Palaeogeography, Palaeoclimatology, Palaeoecology,* 556, 109873. https://doi.org/10.1016/j.palaeo.2020.109873

Perri, F., Scarciglia, F., Apollaro, C. & Marini, L. (2015). Characterization of granitoid profiles in the Sila Massif (Calabria, southern Italy) and reconstruction of weathering processes by mineralogy, chemistry, and reaction path modeling. *Journal of Soils and Sediments*, 15(6), 1351-1372. https://doi.org/10.1007/s11368-014-0856-x

Price, J. R. & Velbel, M. A. (2003). Chemical weathering indices applied to weathering profiles developed on heterogeneous felsic metamorphic parent rocks. *Chemical geology*, 202(3-4), 397-416. https://doi.org/10.1016/j.chemgeo.2002.11.001

Reynolds, R. C. (1980). *Interstratified clay minerals*. In: Brindley, G. W. and Brown, G. (Editors). Crystal Structures of Clay Minerals and their X-ray Identification, Monograph 5, Mineralogical Society, London, 49–303 pp. https://doi.org/10.1180/mono-5.4

Robert, M. & Tessier, D. (1992). *Incipient weathering: some new concepts on weathering, clay formation and organization*. In: Martini, V. & Chesworth, W. (Editors). Developments in Earth Surface Processes (Vol. 2). Elsevier, 71-105 pp. https://doi.org/10.1016/B978-0-444-89198-3.50009-X

Robertson, I. D. & Eggleton, R. A. (1991). Weathering of granitic muscovite to kaolinite and halloysite and of plagioclase-derived kaolinite to halloysite. *Clays and Clay Minerals,* 39(2), 113-126. https://doi.org/10.1346/CCMN.1991.0390201

Rodríguez Fernández, L. R. (1982). *Mapa Geológico Nacional (MAGNA), serie 2ª, primera edición, Eccala 1:50.000 hoja nº127 (Noceda)*. Instituto Geológico y Minero de España (IGME), Madrid.

Romero, R., Robert, M., Elsass, F. & García, C. (1992). Abundance of halloysite neoformation in soils developed from crystalline rocks. Contribution of transmission electron microscopy. *Clay Minerals,* 27(1), 35-46. https://doi.org/10.1180/claymin.1992.027.1.04

Ruxton, B. P. (1968). Measures of the degree of chemical weathering of rocks. *The Journal of Geology*, 76(5), 518-527. https://doi.org/10.1086/627357

Scarciglia, F., Critelli, S., Borrelli, L., Coniglio, S., Muto, F. & Perri, F. (2016). Weathering profiles in granitoid rocks of the Sila Massif uplands, Calabria, southern Italy: New insights into their formation processes and rates. *Sedimentary geology*, 336, 46-67. https://doi.org/10.1016/j.sedgeo.2016.01.015

Senol, H., Tunçay, T. & Dengiz, O. (2016). Geochemical mass-balance, weathering and evolution of soils formed on a Quaternary-age basaltic toposequences. *Solid Earth Discuss* (preprint), 105, 1-22. https://doi.org/10.5194/se-2016-105

Spears, D. (2016). Clay mineralogy of onshore UK Carboniferous mudrocks. *Clay Minerals,* 41(1), 395-416. https://doi.org/10.1180/0009855064110201

Suárez, O., Corretgé, L. G. & Martínez, F. J. (1990). *The West Asturian-Leonese Zone. Distribution and characteristics of the Hercynian metamorphism*. In: Dallmeyer, R. D. & Martínez-García, E. (Editors). Pre-Mesozoic Geology of Iberia, Springer-Verlag, Berlín, 129-133.

Taboada, T. & Garcia, C. (1999). Pseudomorphic transformation of plagioclases during the weathering of granitic rocks in Galicia (NW Spain). *Catena,* 35 (2-4), 291-302. https://doi.org/10.1016/S0341-8162(98)00108-8

Tardy, Y., Bocquier, G., Paquet, H. & Millot, G. (1973). Formation of clay from granite and its distribution in relation to climate and topography. *Geoderma*, 10, 271–284. https://doi.org/10.1016/0016-7061(73)90002-5

Vicente, M. A., Molina, E. & Espejo, R. (1991). Clays in paleoweathering processes: study of a typical weathering profile in the Hercynian basement in the Montes de Toledo (Spain). *Clay Minerals*, 26(1), 81-90. https://doi.org/10.1180/claymin.1991.026.1.08

Vicente, M. A., Elsass, F., Molina, E. & Robert, M. (1997). Palaeoweathering in slates from the Iberian Hercynian Massif (Spain): investigation by TEM of clay mineral signatures. *Clay Minerals*, 32(3), 435-451. https://doi.org/10.1180/claymin.1997.032.3.06

Wagner, R. H. (2004). The Iberian Massif: a Carboniferous assembly. *Journal of Iberian Geology*, 30, 93–108.

White, A. F. & Brantley, S. L. (2003). The effect of time on the weathering of silicate minerals: why do weathering rates differ in the laboratory and field? *Chemical Geology,* 202(3-4), 479-506. https://doi.org/10.1016/j.chemgeo.2003.03.001

White, A. F. & Buss, H. L. (2014). *Natural weathering rates of silicate minerals*. Treatise on geochemistry, Second Edition. Elsevier, Oxford, 115-155.

White, A. F., Bullen, T. D., Schulz, M. S., Blum, A. E., Huntington, T. G. & Peters, N. E. (2001). Differential rates of feldspar weathering in granitic regoliths. *Geochimica et Cosmochimica Acta,* 65(6), 847-869. https://doi.org/10.1016/S0016-7037(00)00577-9

Wilson, M. J. (2004). Weathering of the primary rock-forming minerals: processes, products and rates. *Clay Minerals*, 39(3), 233-266. https://doi.org/10.1180/0009855043930133

Young, G. M. & Nesbitt, H. W. (1998). Processes controlling the distribution of Ti and Al in weathering profiles, siliciclastic sediments and sedimentary rocks. *Journal of Sedimentary research*, 68(3), 448-455. https://doi.org/10.2110/jsr.68.448